

AN APPLICATION OF FLOQUET THEORY TO PREDICTION OF MECHANICAL INSTABILITY

C. E. Hammond
Langley Directorate
U.S. Army Air Mobility R&D Laboratory
NASA Langley Research Center
Hampton, Virginia

Abstract

The problem of helicopter mechanical instability is considered for the case where one blade damper is inoperative. It is shown that if the hub is considered to be nonisotropic the equations of motion have periodic coefficients which cannot be eliminated. However, if the hub is isotropic the equations can be transformed to a rotating frame of reference and the periodic coefficients eliminated. The Floquet Transition Matrix method is shown to be an effective way of dealing with the nonisotropic hub and nonisotropic rotor situation. Time history calculations are examined and shown to be inferior to the Floquet technique for determining system stability. A smearing technique used in the past for treating the one damper inoperative case is examined and shown to yield unconservative results. It is shown that instabilities which occur when one blade damper is inoperative may consist of nearly pure blade motion or they may be similar to the classical mechanical instability.

Notation

c_i lag damping rate
 c_x effective hub damping in x-direction
 c_y effective hub damping in y-direction
 e lag hinge offset
 I_b second mass moment of blade about lag hinge
 k_i lag spring rate
 k_x effective hub stiffness in x-direction
 k_y effective hub stiffness in y-direction
 m_b blade mass
 m_x effective hub mass in x-direction
 m_y effective hub mass in y-direction
 N number of blades in rotor
 P_j characteristic exponent corresponding to j th eigenvalue of the Floquet Transition Matrix

P_x force acting on hub in x-direction
 P_y force acting on hub in y-direction
 S_b first mass moment of blade about lag hinge
 T period of the periodic coefficients,
 $T = 2\pi/\Omega$
 \bar{x}, \bar{y} coordinates of hub in rotating reference frame
 x_c, y_c coordinates of rotor center of mass in fixed reference frame
 x_h, y_h coordinates of hub in fixed reference frame
 x_i, y_i coordinates of elemental blade mass dm in fixed reference frame
 ζ_i lag deflection of i th blade
 η_h defined by Equations (18)
 η_i defined by Equations (7)
 Λ_j j th eigenvalue of the Floquet Transition Matrix
 v_h defined by Equations (18)
 v_o defined by Equations (7)
 ρ distance from lag hinge to elemental blade mass dm
 ψ_i azimuthal location of i th blade
 Ω rotor speed
 ω_h defined by Equations (18)
 ω_{o_i} defined by Equations (7)
 $[A(t)]$ characteristic matrix, periodic with period T
 $[D(t)]$ state matrix, periodic with period T
 $[Q]$ Floquet Transition Matrix
 $[\phi(t)]$ state transition matrix
 $\{z(t)\}$ state vector

Presented at the AHS/NASA Ames Specialists' Meeting on Rotorcraft Dynamics, February 13-15, 1974.

The problem of mechanical instability of helicopters on the ground has been recognized and understood for many years. The analysis by Coleman and Feingold¹ has become the standard reference on this phenomenon although it was not published until many years after the first incidents of mechanical instability, or ground resonance as it is commonly known, were encountered on the early autogyros. The mechanical instability phenomenon is most commonly associated with helicopters having articulated rotors; however, helicopters using the soft-inplane hingeless rotors which have become popular in recent years are also susceptible to this problem. Machines employing these soft-inplane hingeless rotors are also known to experience a similar problem, commonly known as air resonance, which occurs in flight rather than on the ground. The air resonance problem has received much attention in recent years (see, e.g., Refs. 2 and 3).

From the analysis of Reference 1 and others it is known that the ground resonance problem is due primarily to a coupling of the blade inplane motion with the rigid body degrees of freedom of the helicopter on its landing gear. These analyses have shown that with the proper selection of blade lag dampers and landing gear characteristics the problem of mechanical instability can be eliminated within the operating rotor speed range. All of the mechanical instability analyses conducted to date have one assumption in common - all blades are assumed to have identical properties. This is a reasonable assumption under ordinary circumstances; however, the U.S. Army has a requirement on new helicopters which invalidates this assumption. The requirement is that the helicopter be free from ground resonance with one blade damper inoperative. As will be shown later, this one blade damper inoperative requirement has a serious impact on the classical method of analyzing a helicopter for mechanical instability. Further, there is at present no published method available for treating the case where each of the blades is permitted to have different properties. Thus the designer is faced with the dilemma of trying to satisfy the requirement with an analysis method in which one of the basic assumptions is severely violated.

Two methods have been used to circumvent this difficulty. The first of these involves a physical approximation so that the classical analysis becomes applicable. In this approach all blades are still assumed to have identical lag dampers even when one blade damper is removed, but the value of each of the dampers is reduced by the amount c_i/N where N is the number of blades and c_i is the original lag damper rate. As can be seen, with this approach a system is analyzed which is quite different from the actual situation of a rotor with no damping on one blade. The second method which has been used is to reformulate the equations of motion allowing for differing blade characteristics and to obtain the stability characteristics of the system using a time history integration of the equations. This second approach has the drawback that interpretation of stability characteristics from time history calculations is often difficult and open to question. The method

will yield correct results, however, provided the equations are integrated over a sufficiently long time period.

The purpose of this paper is to present a method of obtaining the mechanical stability characteristics directly for a helicopter operating on the ground with one blade damper inoperative. As will be shown later, the equations governing the motion of this system have periodic coefficients. This fact suggests the use of Floquet theory as the means for determining the stability characteristics of the system. In the following, the one-damper-inoperative problem is formulated and the resulting equations are solved using the Floquet Transition Matrix method described by Peters and Hohenemser.⁴ Results obtained using this method are compared with results obtained from the two previously used methods and recommendations are made concerning the future use of the three methods described.

Equations of Motion

The equations of motion for the mechanical instability problem will be formulated using an Eulerian approach. It will be assumed, as is done in Reference 1, that the helicopter on its landing gear can be represented by effective parameters applied at the rotor hub. It will be further assumed that only inplane motions of the hub and blades are important in determining the ground resonance characteristics of the helicopter. Thus the degrees of freedom to be considered consist of two inplane hub degrees of freedom and a lead-lag degree of freedom for each blade in the rotor. The mathematical model to be used in the analysis is shown in Figure 1. Note that in the figure only a typical blade is shown. The analysis will be formulated for a rotor having N blades, and each blade is assumed to have a rotational spring and damper which act about the lag hinge.

The blade equations are developed by summing moments about the lag hinge. The coordinates of the elemental mass dm in the fixed system are

$$\left. \begin{aligned} x_i &= x_h + e \cos \psi_i + \rho \cos(\psi_i + \zeta_i) \\ y_i &= y_h + e \sin \psi_i + \rho \sin(\psi_i + \zeta_i) \end{aligned} \right\} \quad (1)$$

where

$$\psi_i = \Omega t + 2\pi(i-1)/N \quad i = 1, 2, \dots, N$$

These expressions can be differentiated twice with respect to time to yield the accelerations experienced by the differential mass

$$\left. \begin{aligned} \ddot{x}_i &= \ddot{x}_h - e\Omega^2 \cos \psi_i - \rho(\Omega + \dot{\zeta}_i)^2 \cos(\psi_i + \zeta_i) \\ &\quad - \rho \ddot{\zeta}_i \sin(\psi_i + \zeta_i) \\ \ddot{y}_i &= \ddot{y}_h - e\Omega^2 \sin \psi_i - \rho(\Omega + \dot{\zeta}_i)^2 \sin(\psi_i + \zeta_i) \\ &\quad + \rho \ddot{\zeta}_i \cos(\psi_i + \zeta_i) \end{aligned} \right\} \quad (2)$$

Using D'Alembert's principle the summation of moments about the lag hinge can be written as

$$\int \rho \sin(\psi_i + \zeta_i) \ddot{x}_1 dm - \int \rho \cos(\psi_i + \zeta_i) \ddot{y}_1 dm - k_1 \zeta_i - c_1 \dot{\zeta}_i = 0 \quad i = 1, 2, \dots, N \quad (3)$$

where the integrals are evaluated over the length of the blade. Introducing the expressions for \ddot{x}_1 and \ddot{y}_1 and defining the following

$$\left. \begin{aligned} S_b &= \int \rho dm \\ I_b &= \int \rho^2 dm \end{aligned} \right\} \quad (4)$$

the blade equations become

$$\begin{aligned} I_b \ddot{\zeta}_1 + e \Omega^2 S_b \sin \zeta_1 - S_b [\ddot{x}_h \sin(\psi_1 + \zeta_1) - \ddot{y}_h \cos(\psi_1 + \zeta_1)] + k_1 \zeta_1 + c_1 \dot{\zeta}_1 = 0 \end{aligned} \quad (5)$$

$i = 1, 2, \dots, N$

If small displacements are now assumed the blade equations may be linearized to obtain

$$\begin{aligned} \ddot{\zeta}_1 + \eta_1 \dot{\zeta}_1 + (\omega_{o_1}^2 + \Omega^2 v_o^2) \zeta_1 = (v_o^2/e) [\ddot{x}_h \sin \psi_1 - \ddot{y}_h \cos \psi_1] \end{aligned} \quad (6)$$

$i = 1, 2, \dots, N$

where the following parameters have been introduced

$$\left. \begin{aligned} v_o^2 &= e S_b / I_b \\ \omega_{o_1}^2 &= k_1 / I_b \\ \eta_1 &= c_1 / I_b \end{aligned} \right\} \quad (7)$$

Under the assumptions stated earlier the hub equations of motion can be written directly as

$$\left. \begin{aligned} m_x \ddot{x}_h + c_x \dot{x}_h + k_x x_h &= P_x \\ m_y \ddot{y}_h + c_y \dot{y}_h + k_y y_h &= P_y \end{aligned} \right\} \quad (8)$$

where the coefficients on the left side of these equations are the effective hub properties in the x- and y-directions, respectively. The determination of these properties depends on an extensive knowledge of the helicopter inertial characteristics and the stiffness, damping, and geometrical characteristics of the landing gear system. These properties may be determined either by ground shake tests of the helicopter, as suggested in Reference 1, or by direct calculations. The right-hand side of the above equations are the forces acting on the hub due to the fact that the rotor is experiencing accelerations in the x- and y-directions. If the accelerations of the rotor center of mass are \ddot{x}_c and \ddot{y}_c , respectively, the P_x and P_y are given by

$$\left. \begin{aligned} P_x &= -N m_b \ddot{x}_c \\ P_y &= -N m_b \ddot{y}_c \end{aligned} \right\} \quad (9)$$

The equations as written also indicate that in the absence of the rotor the hub degrees of freedom are

uncoupled. This is an approximation, but it is an assumption made in Reference 1 and one generally used in helicopter mechanical stability analyses.

If all blades in the rotor are assumed to have the same mass distribution, the coordinates for the total rotor center of mass may be written as

$$\left. \begin{aligned} x_c &= x_h + \frac{1}{N} \sum_{i=1}^N x_{i_c} \\ y_c &= y_h + \frac{1}{N} \sum_{i=1}^N y_{i_c} \end{aligned} \right\} \quad (10)$$

where x_{i_c} and y_{i_c} are the coordinates of the individual blade center of mass, measured with respect to the hub. If the center of mass of the i th blade is a radial distance ρ_c from the lag hinge

$$\left. \begin{aligned} x_{i_c} &= e \cos \psi_i + \rho_c \cos(\psi_i + \zeta_i) \\ y_{i_c} &= e \sin \psi_i + \rho_c \sin(\psi_i + \zeta_i) \end{aligned} \right\} \quad (11)$$

Making the observation that, for $N > 1$

$$\sum_{k=1}^N \cos \psi_k = \sum_{k=1}^N \sin \psi_k = 0$$

the rotor center of mass coordinates become

$$\left. \begin{aligned} x_c &= x_h - (\rho_c/N) \sum_{i=1}^N \zeta_i \sin \psi_i \\ y_c &= y_h + (\rho_c/N) \sum_{i=1}^N \zeta_i \cos \psi_i \end{aligned} \right\} \quad (12)$$

These expressions may now be differentiated twice with respect to time and the forces P_x and P_y obtained as

$$\left. \begin{aligned} P_x &= -N m_b \ddot{x}_h + S_b \sum_{i=1}^N \left[(\ddot{\zeta}_i - \Omega^2 \zeta_i) \sin \psi_i + 2\Omega \dot{\zeta}_i \cos \psi_i \right] \\ P_y &= -N m_b \ddot{y}_h - S_b \sum_{i=1}^N \left[(\ddot{\zeta}_i - \Omega^2 \zeta_i) \cos \psi_i - 2\Omega \dot{\zeta}_i \sin \psi_i \right] \end{aligned} \right\} \quad (13)$$

The hub equations of motion thus become

$$\left. \begin{aligned} (m_x + N m_b) \ddot{x}_h + c_x \dot{x}_h + k_x x_h &= \\ S_b \sum_{i=1}^N \left[(\ddot{\zeta}_i - \Omega^2 \zeta_i) \sin \psi_i + 2\Omega \dot{\zeta}_i \cos \psi_i \right] & \\ (m_y + N m_b) \ddot{y}_h + c_y \dot{y}_h + k_y y_h &= \\ -S_b \sum_{i=1}^N \left[(\ddot{\zeta}_i - \Omega^2 \zeta_i) \cos \psi_i - 2\Omega \dot{\zeta}_i \sin \psi_i \right] & \end{aligned} \right\} \quad (14)$$

The equations of motion for the system thus consist of $(N + 2)$ coupled second-order differential

equations with the coupling terms having periodic coefficients. The periodic coefficients arise because the blade equations are written in a rotating reference system whereas the hub equations are in a fixed system. As is shown in the Appendix, if all the blades have identical lag springs and lag dampers, the periodic coefficients may be eliminated through the use of multiblade coordinates. The effect of these coordinates is to transform the blade equations from the rotating to the fixed system of reference. The resulting constant coefficient system of equations is the set normally solved in the classical ground resonance analysis. As is shown, however, if the blades are allowed to have different lag springs and dampers, the periodic coefficients cannot be eliminated in the usual manner.

An alternative does exist, however, for eliminating the periodic coefficients even when the blades are allowed to have differing characteristics. The alternative consists of transforming the hub equations into the rotating system of reference. In order to eliminate the periodic coefficients using this approach, the additional assumption must be made that the hub is isotropic. That is

$$\begin{aligned} m_x &= m_y \\ c_x &= c_y \\ k_x &= k_y \end{aligned}$$

This is the approach used in Reference 1 for treating the two-bladed rotor which is another case where the periodic coefficients in the equations of motion cannot be eliminated by transforming the blade equations to the fixed system.

The transformation from fixed to rotating coordinates is given by

$$\left. \begin{aligned} \bar{x} &= x_h \cos \Omega t + y_h \sin \Omega t \\ \bar{y} &= -x_h \sin \Omega t + y_h \cos \Omega t \end{aligned} \right\} \quad (15)$$

Differentiating these expressions allows the following identities to be established

$$\begin{aligned} \dot{x}_h \cos \Omega t + \dot{y}_h \sin \Omega t &= \dot{\bar{x}} - \Omega \bar{y} \\ -\dot{x}_h \sin \Omega t + \dot{y}_h \cos \Omega t &= \dot{\bar{y}} + \Omega \bar{x} \\ \ddot{x}_h \cos \Omega t + \ddot{y}_h \sin \Omega t &= \ddot{\bar{x}} - \Omega^2 \bar{x} - 2\Omega \dot{\bar{y}} \\ -\ddot{x}_h \sin \Omega t + \ddot{y}_h \cos \Omega t &= \ddot{\bar{y}} - \Omega^2 \bar{y} + 2\Omega \dot{\bar{x}} \end{aligned}$$

The hub equations in the rotating system are then obtained by appropriate combinations of the x_h and y_h equations, Equations (14). The resulting equations are given below

$$\begin{aligned} \ddot{\bar{x}} + \eta_h \dot{\bar{x}} + (\omega_h^2 - \Omega^2) \bar{x} - 2\Omega \dot{\bar{y}} - \Omega \eta_h \bar{y} \\ = v_h^2 \sum_{j=1}^N \left[(\ddot{\zeta}_j - \Omega^2 \zeta_j) \sin \frac{2\pi}{N}(j-1) + 2\Omega \dot{\zeta}_j \cos \frac{2\pi}{N}(j-1) \right] \end{aligned} \quad (16)$$

$$\begin{aligned} \ddot{\bar{y}} + \eta_h \dot{\bar{y}} + (\omega_h^2 - \Omega^2) \bar{y} + 2\Omega \dot{\bar{x}} + \Omega \eta_h \bar{x} \\ = -v_h^2 \sum_{j=1}^N \left[(\ddot{\zeta}_j - \Omega^2 \zeta_j) \cos \frac{2\pi}{N}(j-1) - 2\Omega \dot{\zeta}_j \sin \frac{2\pi}{N}(j-1) \right] \end{aligned} \quad (17)$$

where the following parameters have been introduced

$$\left. \begin{aligned} v_h^2 &= S_b / (m_x + Nm_b) \\ \omega_h^2 &= k_x / (m_x + Nm_b) \\ \eta_h &= c_x / (m_x + Nm_b) \end{aligned} \right\} \quad (18)$$

Introducing the rotating coordinates into the blade equations, Equations (6), results in

$$\begin{aligned} \ddot{\zeta}_j + \eta_j \dot{\zeta}_j + (\omega_{oj}^2 + \Omega^2 v_{oj}^2) \zeta_j \\ = (v_{oj}^2 / e) \left[(\ddot{\bar{x}} - \Omega^2 \bar{x} - 2\Omega \dot{\bar{y}}) \sin \frac{2\pi}{N}(j-1) \right. \\ \left. - (\ddot{\bar{y}} - \Omega^2 \bar{y} + 2\Omega \dot{\bar{x}}) \cos \frac{2\pi}{N}(j-1) \right] \end{aligned} \quad (19)$$

$j = 1, 2, \dots, N$

Since modern helicopters do not in general have isotropic hubs, the above equations can only be used to approximate the effects of a nonisotropic rotor. They are, however, easily solved for the stability characteristics of the system and thus they might be used to obtain a first approximation to the mechanical stability boundary for a helicopter with one blade damper inoperative.

From the foregoing discussion it can be seen that if either the rotor or the hub is isotropic, the mechanical stability characteristics of the system may be obtained using conventional techniques. If both the rotor and hub are nonisotropic the equations of motion of the system contain periodic coefficients and thus the standard eigenvalue techniques cannot be used to determine whether the system is stable or unstable. It is the purpose of this paper to demonstrate that Floquet theory can be used to analyze this general situation of a nonisotropic rotor coupled with a nonisotropic hub.

Solution of the Equations

If the periodic coefficients in the equations of motion are eliminated by assuming either an isotropic rotor or an isotropic hub, the stability of the system can be determined using standard eigenvalue techniques. The general case of a nonisotropic rotor coupled with a nonisotropic hub will be treated using Floquet techniques as described by Peters and Hohenemser,⁴ and Hohenemser and Yin.⁵ A brief description of the technique will be presented here for the sake of completeness.

In state vector rotation the free motions of the system may be written as

$$\{\dot{\mathbf{z}}\} = [D(t)]\{\mathbf{z}\} \quad (20)$$

where the state variables for the problem being considered consist of

$$\zeta_1, \zeta_2, \dots, \zeta_N, x_h, y_h, \dot{\zeta}_1, \dot{\zeta}_2, \dots, \dot{\zeta}_N, \dot{x}_h, \dot{y}_h$$

and the equations which describe the motions of the system are Equations (6) and (14). The matrix $[D(t)]$ is periodic with period T and for the mechanical stability problem $T = 2\pi/\Omega$.

Floquet's theorem states that the solution to the above system of equations has the form

$$\{z\} = [A(t)] \{ \alpha e^{(\lambda+i\omega)t} \} \quad (21)$$

where $[A(t)]$ is the characteristic matrix and is also periodic with period T . The column of initial conditions $\{z(0)\}$ is used in determining $\{\alpha\}$ as

$$\{\alpha\} = [A(0)]^{-1} \{z(0)\} \quad (22)$$

The matrix $[A(0)]$, the modal damping λ , and the modal frequency ω are determined from the Floquet Transition Matrix $[Q]$ which is defined by the equation

$$\{z(T)\} = [Q] \{z(0)\} \quad (23)$$

for all sets of initial conditions $\{z(0)\}$. It is shown in References 4 and 5 that the eigenvalues Λ_j of the matrix $[Q]$ can be used to determine λ_j and ω_j since

$$\Lambda_j = e^{(\lambda_j+i\omega_j)T} \quad (24)$$

and the modal matrix of $[Q]$ is just $[A(0)]$. The characteristic matrix $[A(t)]$ is then shown to be given by

$$[A(t)] = [\phi(t)][A(0)] \left[e^{-(\lambda+i\omega)t} \right] \quad (25)$$

where the state transition matrix $[\phi(t)]$ is defined by

$$\{z(t)\} = [\phi(t)] \{z(0)\} \quad (26)$$

The characteristic multipliers Λ_j of the system are uniquely defined since the matrix $[Q]$ is real; however, only the real parts of the characteristic exponents $p_j = \lambda_j + i\omega_j$ are defined uniquely since

$$p_j = \frac{1}{T} (\ln |\Lambda_j| + i \arg \Lambda_j) \quad (27)$$

The imaginary part can only be determined within an integer multiple of $2\pi/T$. This indeterminacy of the ω_j causes no particular difficulty if one is only interested in the stability of the system. However, if one is interested in understanding the mechanism involved in any instability which might be found, this indeterminacy can be quite troublesome.

The Floquet Transition Matrix which is the basic element needed in the stability analysis is easily determined by a numerical integration of the equations of motion over one period T . If one desires to compute the characteristic functions

$[A(t)]$ the matrix $[\phi(t)]$ is saved at each time point in the numerical integration to obtain $[Q]$. For the calculations of this paper, the fourth order Runge-Kutta method with Gill coefficients⁶ was used for the numerical integration.

A comment is in order concerning the characteristic functions $[A(t)]$. The matrix $[A(t)]$ is a complex valued matrix and is determined at as many time points as desired. The computation of these functions can be relatively expensive and interpretation can be difficult. The interpretation is made easier by the procedure outlined in Reference 5 for converting the complex functions into real functions which may be plotted as functions of time. The scheme used is essentially the same as that used when it is desired to plot as a function of time the modes of a system having constant coefficients. That is, for a conjugate pair of characteristic exponents

$$p_j = \lambda_j + i\omega_j$$

$$\bar{p}_j = \lambda_j - i\omega_j$$

the characteristic functions are also conjugate pairs. Thus the real modal function column for this conjugate pair of characteristic exponents will be given by

$$\{z_j(t)\} = \{A_j(t)\} e^{(\lambda_j+i\omega_j)t} + \{\bar{A}_j(t)\} e^{(\lambda_j-i\omega_j)t} \quad (28)$$

where $\{A_j(t)\}$ is the j th column of $[A(t)]$ and $\{\bar{A}_j(t)\}$ is the complex conjugate of this column. The purpose in performing these manipulations is to be able to plot the modal functions to determine the relative magnitudes and phases of the various degrees of freedom in each mode. A discussion of this technique as it applies to constant coefficient systems is given by Meirovitch.⁷ In this paper the $\exp(\lambda_j t)$ is omitted from the above equation since it is simply a constant which multiplies each component of the mode and causes each component to damp at the same rate. Thus the plots of the characteristic functions which are presented later in the paper will appear to be neutrally damped.

In making the calculations for this paper it was found that the output from the calculation of the modal functions became so voluminous and these calculations became so expensive that the modal functions were only computed for selected points. Generally a sweep of rotor speed was made and the results examined. If an unstable region was indicated the rotor speed corresponding to the maximum positive λ_j was rerun and the modal functions calculated.

Discussion of Results

In order to demonstrate the application of the above-mentioned techniques and to obtain a general understanding of the effect of one blade damper inoperative on mechanical stability, a set of parameters were chosen. The parameters in the

mechanical stability analysis were chosen so as to be in the general range of interest for a single rotor helicopter and were such that the system was stable with all dampers functioning up to a rotor speed of 400 rpm. The parameter values chosen for the calculations are shown in Table 1.

The parameters presented in Table 1 correspond to an isotropic rotor and a nonisotropic hub. In the following discussion results are presented for the case of an isotropic hub coupled with a nonisotropic rotor and a nonisotropic hub coupled with an isotropic rotor as well as the case of interest which involves a nonisotropic hub coupled with a nonisotropic rotor. When an isotropic hub is mentioned, this means that the hub parameters in both the x- and y-directions were assigned the values shown in Table 1 for the x-direction. An isotropic rotor implies that all dampers are operational and a nonisotropic rotor is meant to indicate that the lag damper has been removed from blade number 1. The analysis has been formulated in such a way that any number of blade lag dampers or lag springs may be removed to make the rotor nonisotropic. The results presented here, however, only involve the removal of the lag damper from one blade.

The case of an isotropic hub was first run in an effort to become familiar with the nonisotropic rotor results before proceeding with the more complicated Floquet analysis. The isotropic hub permits the equations to be transformed into the rotating reference frame and results in a system of equations with constant coefficients, Equations (16), (17), and (19), even with a nonisotropic rotor.

Figure 2 shows the results of the calculations for the isotropic hub with all blade dampers working. Note that since the equations were solved in the rotating system, the frequencies in the lower portion of Figure 2 are plotted in the rotating system. The numbers attached to the different modes in Figure 2 and in subsequent similar figures have no significance other than to provide a label for the various modes. In Figure 2 the dashed lines represent the uncoupled hub modes. The uncoupled rotor modes follow along the curves labeled 1,2 which also represent, in the terminology of Reference 5, the rotor collective modes. Note that the uncoupled blade frequencies are zero for rotor speeds less than about 65 rpm. This is due to the fact that the blades are critically damped for these low rotor speeds. At the higher rotor speeds modes 3 and 4 are essentially rotor modes and modes 5 and 6 are essentially hub modes. At the lower speeds, however, due to the coupling between rotor and hub, mode 4 changes to a hub mode and mode 5 changes to a blade mode. Note from the damping plot that all the modes indicate stability over the entire rotor speed range.

The results for one blade damper inoperative and an isotropic hub are plotted in Figure 3. Note that the removal of a blade damper has caused the appearance of a mode which was not present in Figure 2, namely the mode labeled 3 in Figure 3,

and that this mode exhibits a mild instability between 160 and 200 rpm. At rotor speeds below about 100 rpm this mode has a frequency which corresponds to the uncoupled frequency of the blade which has no damper. At rotor speeds above 100 rpm this mode begins to deviate in frequency from the uncoupled frequency. Another interesting point is that mode 1 in Figure 3 is precisely the same as the collective modes of Figure 2, and in Figure 3 there is only one such mode. Thus it appears that the unstable mode in Figure 3 has evolved from one of the two collective modes shown in Figure 2 because of the removal of one of the blade dampers.

A time history calculation was made for the point of maximum instability in Figure 3 which occurs at approximately 175 rpm. The results of the time history calculation are shown in Figure 4. These results were obtained using the same integration scheme as that used for generating the Floquet Transition Matrix. The top portion of the figure represents the individual blade lag motions whereas the lower portion represents the hub response in the x- and y-directions. Note from the figure that each of the degrees of freedom was given an initial displacement but the initial velocities were zero. The equations were integrated for 17 rotor revolutions. The figure indicates the blades which have lag dampers are well damped, but the blade on which the damper is inoperative experiences large lag excursions. Also, the hub motions, although not large, do not appear to have a high degree of damping. From the time history one would conclude that the system is stable since the motions of the various degrees of freedom do not appear to be increasing in amplitude with increasing time. The eigenvalue analysis has shown, however, that an instability exists. The problem with the time history calculations is, of course, that the equations of motion have not been integrated over a sufficiently long time period for the initial conditions chosen. Herein lies the difficulty with using the time history approach for calculating the stability characteristics of systems. One can never be sure if a sufficiently long integration period has been used, and the choice of initial conditions which will minimize the integration time required is a trial and error process. It has been observed on an analog computer that for the ground resonance problem the choice of initial conditions has a strong bearing on the conclusion inferred from the time history traces. The time history integration is also much more time consuming on the digital computer than the eigenvalue analysis. The time to generate Figure 4 which is for only one rotor speed was much greater than the time required to generate the eigenvalue results for all of Figure 3. It is thus concluded that whenever it is at all possible the eigenvalue approach to stability calculation is to be desired over the time history approach.

Having examined the case of one blade damper inoperative on an isotropic hub, the next logical step is to examine the more realistic situation of a nonisotropic hub. Before examining the one damper inoperative situation it was first desired

to confirm that the system was stable with all dampers working. The modal damping and frequency of the various modes with all dampers working and a nonisotropic hub are shown in Figure 5. As can be seen from the damping plot, all the modes are stable. In this case the equations of motion are solved in the fixed frame of reference and hence the frequencies are plotted in this frame. The dashed lines on the frequency plot represent the uncoupled system: the horizontal dashed lines being the hub modes and the slanted dashed lines being the rotor modes. Note that because the rotor modes become critically damped at low rotor speeds the two uncoupled rotor frequencies come together before reaching the origin. The uncoupled rotor lines also represent the collective modes for the rotor. These modes are completely uncoupled from the other modes and hence are not included in the eigenvalue analysis of the nonisotropic hub coupled with an isotropic rotor. The damping for the collective modes is exactly the same as that shown for modes 1,2 in Figure 2.

The validity of the Floquet analysis was verified by comparing results from this analysis with results from both the rotating system analysis (isotropic hub) and from the fixed system analysis (isotropic rotor). In each case the results from the Floquet analysis were identical to results from the other analyses.

Having thus established the validity of the Floquet analysis, results were obtained for the nonisotropic hub and one blade damper inoperative. These results are shown in Figure 6. Note that these results are very much similar to those shown in Figure 5 except that, as was the case with the isotropic hub and one blade damper inoperative, there are additional modes introduced. Also indicated is a relatively strong instability between 210 and 305 rpm. The frequencies of the additional modes which are introduced correspond, at low rotor speeds, to the frequencies of the uncoupled blade which has no damper. In the rotor speed range where the instability occurs, however, the frequency deviates from the uncoupled value as indicated by the mode labeled 3. In this range and at higher rotor speeds the mode labeled 5 is nearer the uncoupled blade frequency. It thus appears that for this case the instability is more a coupled rotor hub mode than a pure blade mode as was indicated for the isotropic hub.

This conjecture is further strengthened by an examination of the modal functions. The modal functions for a rotor speed of 255 rpm, which is the point of maximum instability, are shown in Figure 7. The functions are plotted over a time period corresponding to one rotor revolution. Note from this figure that blade 1, the blade without a damper, has a significantly higher contribution to the mode than the other blades. Also from the plot of hub response it can be seen that the participation of the lateral hub degree of freedom, which has the higher of the uncoupled hub frequencies shown on Figure 6, is considerable. It is thus concluded from Figures 5 and 6 that the

one damper inoperative situation can lead to a classical mechanical instability.

Time history traces for this same condition are shown in Figure 8. These traces show the same general trends as observed in the case of the isotropic hub, that is, a large response of the blade having no damper and moderate responses from the other blades and the hub degrees of freedom. Again the time history traces are inconclusive regarding the stability of the system.

One of the methods used in the past for treating the one blade damper inoperative case involves a smearing of the total blade damping. The reasoning for this approach is as follows. If the rotor has N blades then the total damping available in the rotor is Nc_1 where c_1 is the damping on one blade. If one damper is removed, the total damping becomes $(N - 1)c_1$. Thus, using this approach, each blade in the rotor would be treated as if it had a lag damper equal to $c_1(N - 1)/N$.

After an examination of the preceding one damper inoperative results it would be expected that this approach would lead to unconservative results. This is due to the fact that the instabilities encountered in the previous results involved large motions of the blade which had no damper. The smearing technique results in damping, which is not greatly different from the original value, being applied to each blade and thus the true situation is not adequately modeled.

To illustrate this method, the nonisotropic hub case was analyzed using the smearing approach. The results from these calculations are shown in Figure 9. Note that although mode 3 becomes lightly damped the system remains stable throughout the rotor speed range considered. The fact that mode 3 approaches instability is attributable to the fact that this mode was not heavily damped in the original calculations. A run of the isotropic hub case, where all the modes were originally well damped, indicated that the smearing technique resulted in well damped modes for one blade damper removed. The smearing technique is thus not recommended for treating the one blade damper inoperative situation since it leads to unconservative results.

Since one way for eliminating the classical mechanical instability is to increase the blade damping, it was decided to attempt this approach on the instability indicated in Figure 6. The approach was to leave the damping identically zero on one blade and increase the damping on the remaining three blades. The results of this series of calculations are shown in Figure 10 where the region of instability is presented as a function of blade lag damping and rotor speed. As can be seen from the figure, increasing the blade damping on three of the blades has very little effect on the stability boundaries when one blade has zero damping. This result was somewhat expected since from the previous calculations it was observed

that the blade with zero damping responds more or less independently of the other blades in the rotor.

During the increased damping calculations no attempt was made to determine whether or not the nature of the instability had changed. That is, whether the instability had changed from one involving both blade and hub motion to one consisting of primarily blade motion with only small amounts of hub motion. Further delving into possible corrective actions for the instability which occurs with one blade damper inoperative was beyond the scope of this paper and thus more research is needed to determine how the instability may be eliminated.

Conclusions

There are several conclusions which may be inferred from the preceding results. First of all, the fact that a helicopter is free from mechanical instability with all blade dampers working does not guarantee that it will be free of instabilities with one blade damper inoperative. The instability encountered with one blade damper inoperative may be a blade mode instability or it may be the classical mechanical instability.

The Floquet Transition Matrix method can be used effectively in examining the mechanical stability characteristics of helicopters with one blade damper inoperative. When both the hub and rotor are considered to be nonisotropic, the equations of motion contain periodic coefficients and the Floquet approach provides an efficient means for dealing with this situation. Since the Floquet approach yields the stability characteristics directly, it furnishes a more desirable approach to stability problems than time history calculations.

Time history calculations can lead to erroneous conclusions relative to the determination of system stability. The erroneous conclusions stem primarily from the fact that the time history calculations require considerable computer time and the tendency is to integrate over as short a time period as possible. Thus, if the initial conditions are not chosen properly, the time history traces may still contain transients when the integration is terminated. The time history approach to stability problems is thus recommended only when no other recourse is available, and then several different combinations of initial conditions and integration periods should be examined before making a conclusion regarding stability.

The smearing approach which has been used in the past for treating the one blade damper inoperative situation leads to unconservative results. Therefore, this method is considered to be an unacceptable means for determining stability under these conditions.

References

1. Coleman, R. P., and Feingold, A. M., THEORY OF SELF-EXCITED MECHANICAL OSCILLATIONS OF HELICOPTER ROTORS WITH HINGED BLADES, NACA Report 1351, 1958.
2. Donham, R. E., Cardinale, S. V., and Sachs, I. B., GROUND AND AIR RESONANCE CHARACTERISTICS OF A SOFT IN-PLANE RIGID-ROTOR SYSTEM, Journal of the American Helicopter Society, Vol. 14, No. 4, October 1969, pp. 33-41.
3. Lytwyn, R. T., Miao, W., and Woitsch, W., AIRBORNE AND GROUND RESONANCE OF HINGELESS ROTORS, Journal of the American Helicopter Society, Vol. 16, No. 2, April 1971, pp. 2-9.
4. Peters, D. A., and Hohenemser, K. H., APPLICATION OF THE FLOQUET TRANSITION MATRIX TO PROBLEMS OF LIFTING ROTOR STABILITY, Journal of the American Helicopter Society, Vol. 16, No. 2, April 1971, pp. 25-33.
5. Hohenemser, K. H., and Yin, S. K., SOME APPLICATIONS OF THE METHOD OF MULTIBLADE COORDINATES, Journal of the American Helicopter Society, Vol. 17, No. 3, July 1972, pp. 3-12.
6. Carnahan, B., Luther, H. A., and Wilkes, J. O., Applied Numerical Methods, John Wiley & Sons, Inc., New York, 1969.
7. Meirovitch, L., Analytical Methods in Vibrations, The Macmillan Company, New York, 1967, p. 411.

Appendix

If the rotor is considered to be isotropic the periodic coefficients appearing in the equations of motion can be eliminated through the use of multiblade coordinates similar to those described in Reference 1. These coordinates essentially transform the blade degrees of freedom into a fixed reference frame. The transformations are given by

$$\left. \begin{aligned} \xi_I &= \sum_{i=1}^N \zeta_i \sin \psi_i \\ \xi_{II} &= \sum_{i=1}^N \zeta_i \cos \psi_i \end{aligned} \right\} \quad (A1)$$

Differentiating these expressions leads to the establishment of the following identities

$$\left. \begin{aligned} \sum_{i=1}^N \dot{\zeta}_i \sin \psi_i &= \dot{\xi}_I - \Omega \xi_{II} \\ \sum_{i=1}^N \dot{\zeta}_i \cos \psi_i &= \dot{\xi}_{II} + \Omega \xi_I \end{aligned} \right\} \quad (A2)$$

$$\left. \begin{aligned} \sum_{i=1}^N \ddot{\zeta}_i \sin \psi_i &= \ddot{\xi}_I - \Omega^2 \xi_I - 2\Omega \dot{\xi}_{II} \\ \sum_{i=1}^N \ddot{\zeta}_i \cos \psi_i &= \ddot{\xi}_{II} - \Omega^2 \xi_{II} + 2\Omega \dot{\xi}_I \end{aligned} \right\}$$

It can be seen from these identities that the transformation is made by multiplying the blade equations, Equations (6), by either $\sin \psi_i$ or $\cos \psi_i$ and adding the equations. Crucial to this operation is the ability to remove the η_i and $\omega_{O_i}^2$ from the summations. This can only be done if all the blades have identical lag springs and lag dampers. If one or more of the blades have differing characteristics, the η_i and/or $\omega_{O_i}^2$ cannot be factored from the summation and hence the identities above cannot be applied. Thus, if one or more of the blades are permitted to have different lag springs or lag dampers, the periodic coefficients cannot be eliminated using the procedure described in this Appendix.

If Equations (6) are first multiplied by $\cos \psi_i$ and summed and then multiplied by $\sin \psi_i$ and summed, the following equations are obtained after introduction of the identities (A2)

$$\begin{aligned} \ddot{\xi}_{II} + \eta_i \dot{\xi}_{II} - \left[\Omega^2(1 - v_o^2) - \omega_{O_i}^2 \right] \xi_{II} + 2\Omega \dot{\xi}_I \\ + \Omega \eta_i \xi_I = (v_o^2/e) \left[\ddot{x}_h \sum_{i=1}^N \sin \psi_i \cos \psi_i \right. \\ \left. - \ddot{y}_h \sum_{i=1}^N \cos^2 \psi_i \right] \end{aligned} \quad (A3)$$

$$\begin{aligned} \ddot{\xi}_I + \eta_i \dot{\xi}_I - \left[\Omega^2(1 - v_o^2) - \omega_{O_i}^2 \right] \xi_I - 2\Omega \dot{\xi}_{II} \\ - \Omega \eta_i \xi_{II} = (v_o^2/e) \left[\ddot{x}_h \sum_{i=1}^N \sin^2 \psi_i \right. \\ \left. - \ddot{y}_h \sum_{i=1}^N \sin \psi_i \cos \psi_i \right] \end{aligned}$$

Making the following observations that for $N > 2$

$$\begin{aligned} \sum_{i=1}^N \sin \psi_i \cos \psi_i &= 0 \\ \sum_{i=1}^N \cos^2 \psi_i &= \sum_{i=1}^N \sin^2 \psi_i = N/2 \end{aligned}$$

the equations become

$$\left. \begin{aligned} \ddot{\xi}_{II} + \eta_i \dot{\xi}_{II} - \left[\Omega^2(1 - v_o^2) - \omega_{O_i}^2 \right] \xi_{II} + 2\Omega \dot{\xi}_I \\ + \Omega \eta_i \xi_I = -(Nv_o^2/2e) \ddot{y}_h \\ \ddot{\xi}_I + \eta_i \dot{\xi}_I - \left[\Omega^2(1 - v_o^2) - \omega_{O_i}^2 \right] \xi_I - 2\Omega \dot{\xi}_{II} \\ - \Omega \eta_i \xi_{II} = (Nv_o^2/2e) \ddot{x}_h \end{aligned} \right\} \quad (A4)$$

These two equations describe the rotor motions in the fixed frame of reference. In terms of the variables described by Equations (A1) the hub equations, Equations (14), become

$$\left. \begin{aligned} (m_x + Nm_b) \ddot{x}_h + c_x \dot{x}_h + k_x x_h &= S_b \ddot{\xi}_I \\ (m_y + Nm_b) \ddot{y}_h + c_y \dot{y}_h + k_y y_h &= -S_b \ddot{\xi}_{II} \end{aligned} \right\} \quad (A5)$$

The stability of the rotor-hub system can now be determined using Equations (A4) and (A5) which have constant coefficients. This set of equations or a set similar to it is the one normally used in helicopter mechanical stability analyses.

As a final observation, note that if the blade equations, Equations (6), are simply summed, the following equation

$$\ddot{\xi}_o + \eta_i \dot{\xi}_o + (\omega_{O_i}^2 + \Omega^2 v_o^2) \xi_o = 0 \quad (A6)$$

is obtained, where

$$\xi_o = \sum_{i=1}^N \zeta_i \quad (A7)$$

This equation represents the rotor collective mode and it may be observed that this equation is completely decoupled from the hub degrees of freedom. Hence, the collective mode cannot influence the stability of the system and it is therefore not normally included in the mechanical stability analysis.

TABLE 1. PARAMETERS USED IN THE SAMPLE CALCULATIONS

Number of blades	4
Blade mass, m_b	6.5 slugs (94.9 kg)
Blade mass moment, S_b	65.0 slug-ft (289.1 kg-m)
Blade mass moment of inertia, I_b	800.0 slug-ft ² (1084.7 kg-m ²)
Lag hinge offset, e	1.0 ft (0.3048 m)
Lag spring, k_i	0.0 ft-lb/rad (0.0 m-N/rad)
Lag damper, c_i	3000.0 ft-lb-sec/rad (4067.5 m-N-s/rad)
Hub mass, m_x	550.0 slugs (8026.6 kg)
Hub mass, m_y	225.0 slugs (3283.6 kg)
Hub spring, k_x	85000.0 lb/ft (1240481.8 N/m)
Hub spring, k_y	85000.0 lb/ft (1240481.8 N/m)
Hub damper, c_x	3500.0 lb-sec/ft (51078.7 N-s/m)
Hub damper, c_y	1750.0 lb-sec/ft (25539.3 N-s/m)

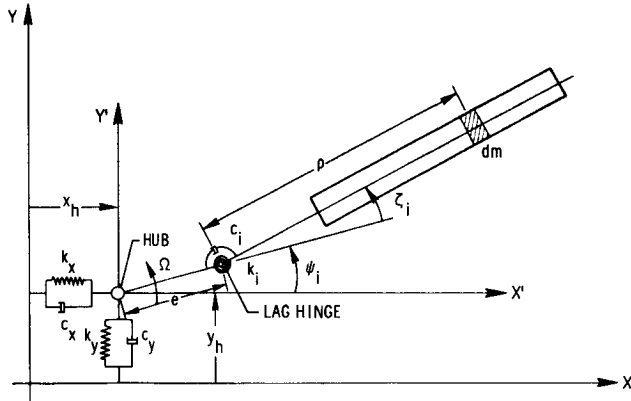


Figure 1. Mathematical representation of the rotor and hub.

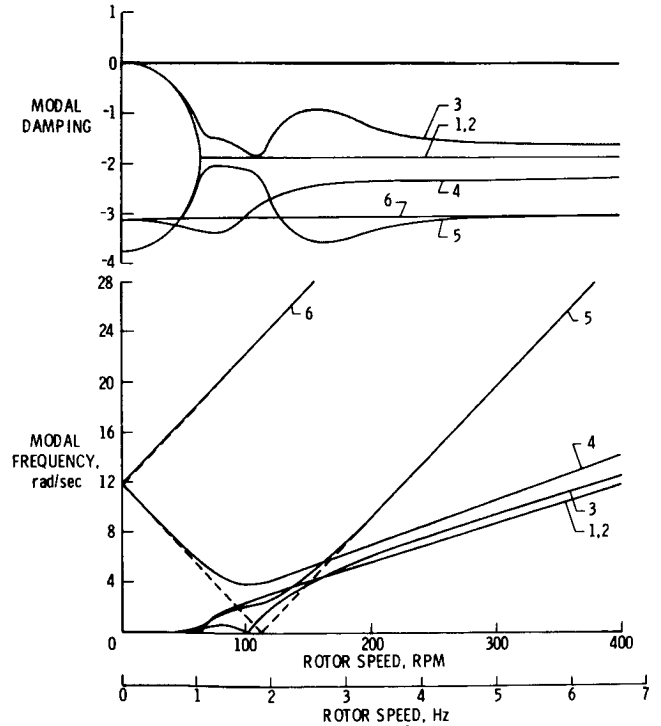


Figure 2. Modal damping and frequencies for isotropic hub, all blade dampers working. Frequencies plotted in the rotating system.

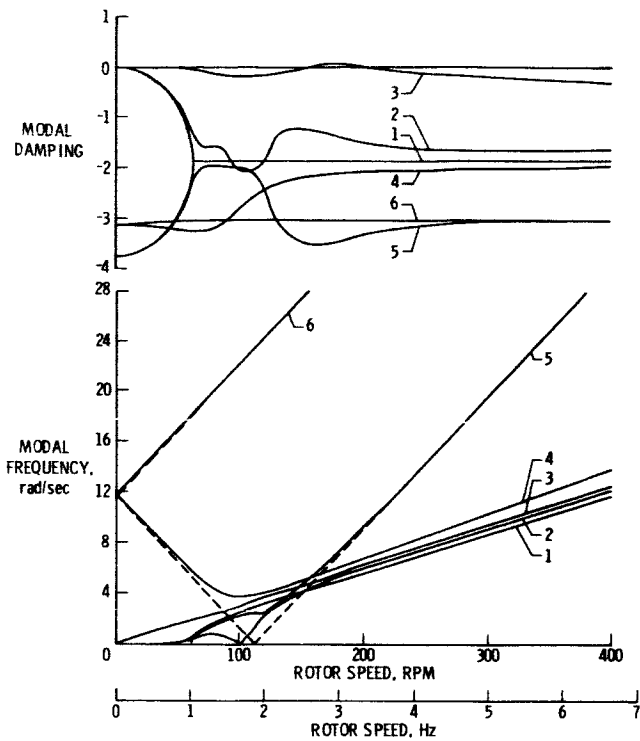


Figure 3. Modal damping and frequencies for isotropic hub, one blade damper inoperative. Frequencies plotted in the rotating system.

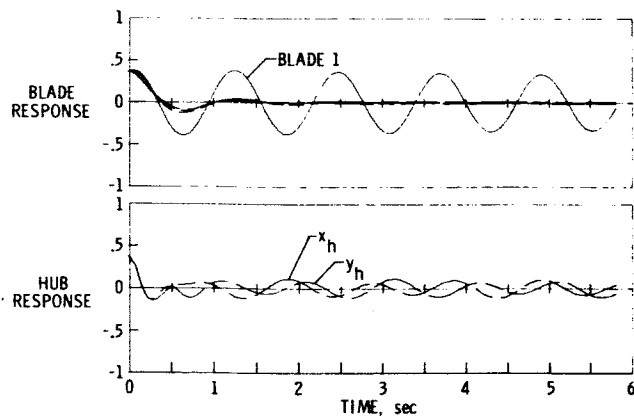


Figure 4. Time history calculations for isotropic hub, one blade damper inoperative, $\Omega = 175$ rpm.

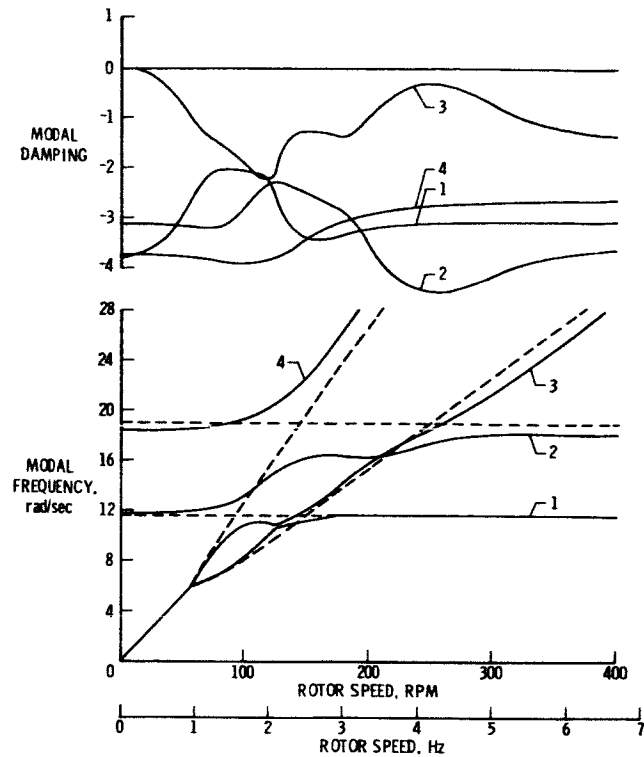


Figure 5. Modal damping and frequencies for non-isotropic hub, all blade dampers working. Frequencies plotted in the fixed system.

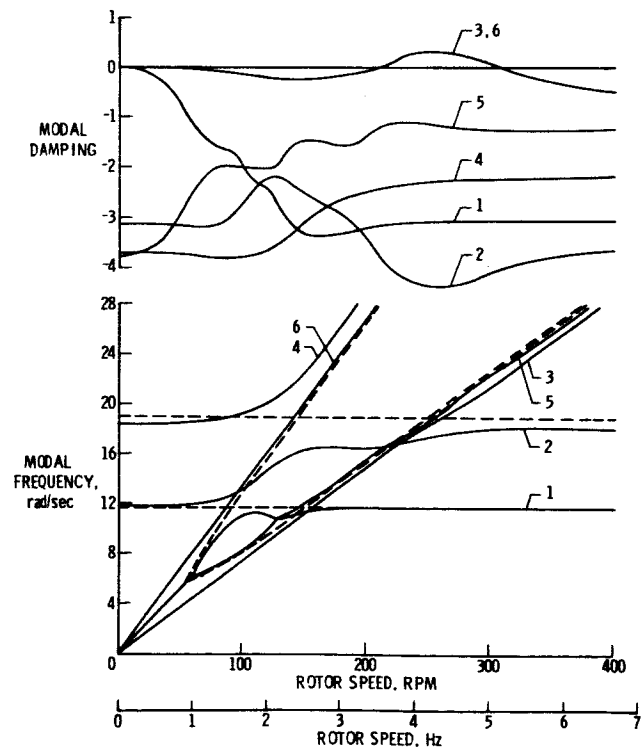


Figure 6. Modal damping and frequencies for non-isotropic hub, one blade damper inoperative. Frequencies plotted in the fixed system.

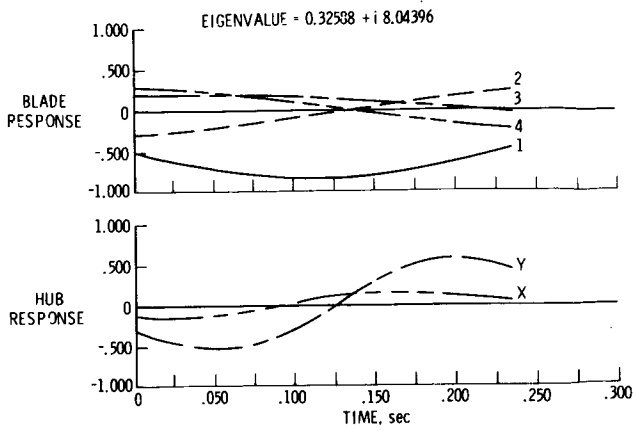


Figure 7. Modal functions for nonisotropic hub, one blade damper inoperative, $\Omega = 255$ rpm.

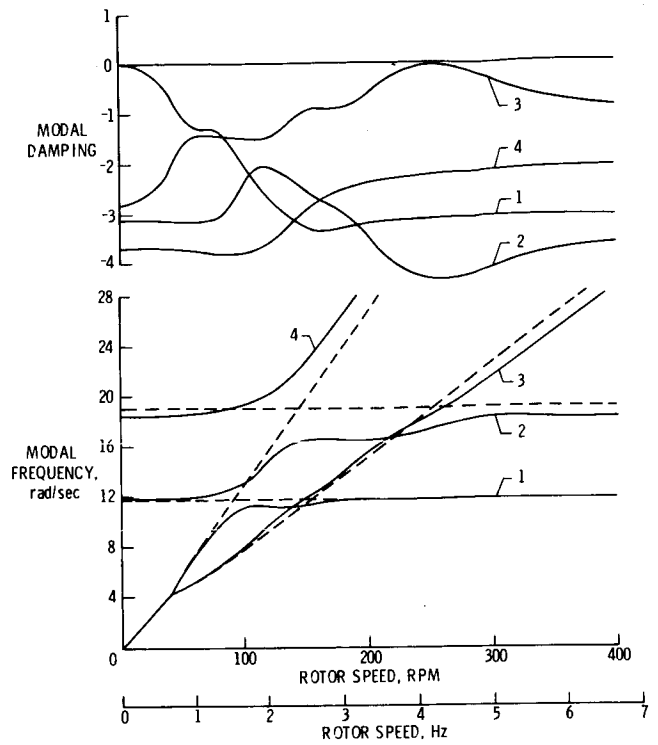


Figure 9. Modal damping and frequencies obtained for nonisotropic hub, one blade damper inoperative, using the smearing technique.

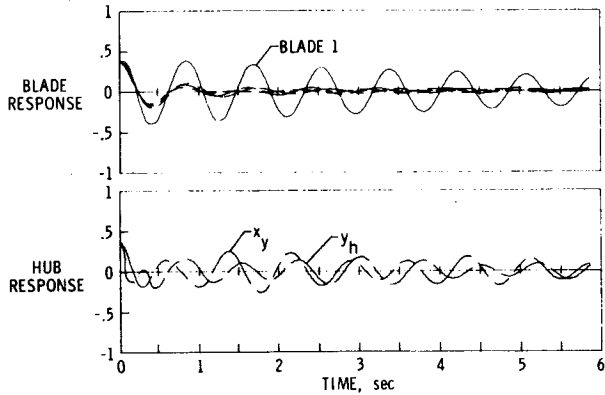


Figure 8. Time history calculations for nonisotropic hub, one blade damper inoperative, $\Omega = 255$ rpm.

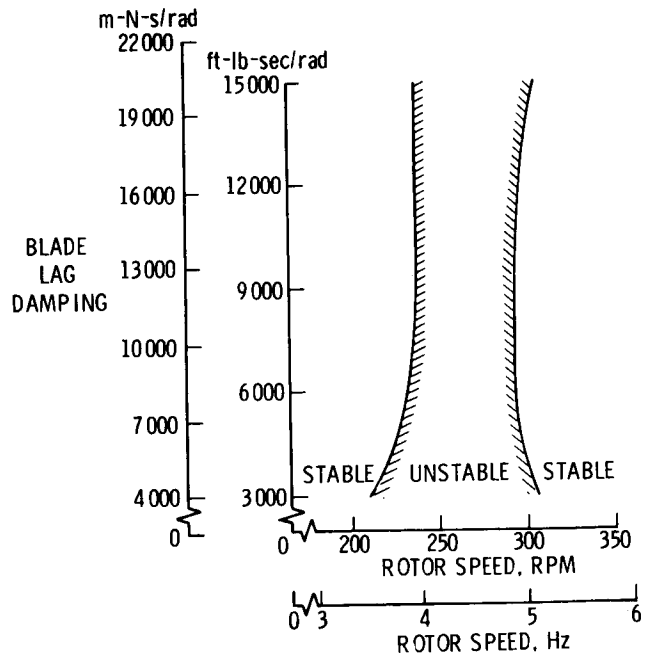


Figure 10. Instability region as a function of blade lag damping for the nonisotropic hub and one blade damper inoperative.